Journal of Catalysis **212,** 112–118 (2002)
doi:10.1006/jcat.2002.3764

RESEARCH NOTE

Production of Hydrogen by Partial Oxidation of Methanol over a Cu/ZnO/Al_2O_3 Catalyst: Influence of the Initial State of the Catalyst on the Start-Up Behaviour of the Reformer

R. M. Navarro, M. A. Peña, and J. L. G. Fierro[1]

Instituto de Catálisis y Petroleoquímica, CSIC, Campus UAM, Cantoblanco, 28049 Madrid, Spain

Received April 19, 2002; revised June 17, 2002; accepted July 29, 2002

The temperature-programmed start-up of a methanol reformer for the production of hydrogen by partial oxidation of methanol, using air as oxidant, was studied over a Cu/ZnO/Al_2O_3 sample in its oxidised, reduced, and reduced + air-exposed states. The temperature at which the reaction starts was shifted to higher values when the degree of surface oxidation increased: oxidised sample $\gg$ reduced sample > reduced + air-exposed sample. Conversely, the same product selectivity is observed irrespective of the initial state of the samples. Methanol partial oxidation over the oxidised sample was accompanied by concomitant surface reduction. This reduction process leads to surface reconstruction with a higher methanol decomposition capacity than that corresponding to prereduced counterparts. These differences appear to be related to changes in the number, but not in the characteristics, of the active sites induced by the different reduction potentials of the reacting gases. For consecutive start-ups, the reaction-reduced catalyst behaves identically to the prereduced counterparts. These observations point to the central role of lattice oxygen during the restructuring of the catalyst surface under reaction conditions. © 2002 Elsevier Science (USA)

Key Words: **fuel cell; hydrogen production; methanol partial oxidation; Cu/ZnO/Al_2O_3 catalyst; methanol reformer; start-up.**

1. INTRODUCTION

Hydrogen gas is an excellent energy vector when used directly as a fuel in internal combustion engines (1) or, indirectly to supply electricity using polymer electrolyte fuel cells. Nevertheless, the use of H_2 gas for mobile fuel cell applications is hindered by problems of storage, safety, refueling, etc. These problems can be overcome by the production of hydrogen on board the vehicle from a suitable high energy/density liquid fuel, such as methanol. Hydrogen can be obtained directly from methanol by three different processes (2): thermal decomposition (TDM) (Eq. [1]), partial oxidation of methanol (POM, Eq. [2]), and steam reforming (SMR, Eq. [3]). The overall processes summarised in Eqs. [1]–[3] are a complex convolution of elementary steps that involve several organic intermediates.

$$\text{TDM}: CH_3OH \rightarrow 2H_2 + CO\ (\Delta H^0 = +90.5\ \text{kJ/mol}) \quad [1]$$

$$\text{POM}: CH_3OH + 1/2\,O_2 \rightarrow 2H_2 + CO_2\ (\Delta H^0 = -191.9\ \text{kJ/mol}) \quad [2]$$

$$\text{SMR}: CH_3OH + H_2O \rightarrow 3H_2 + CO_2\ (\Delta H^0 = +49.8\ \text{kJ/mol}). \quad [3]$$

In the case of hydrogen for nonstationary applications, POM and OMR has shown advantages over the endothermic SMR in regard to kinetic aspects, reactor start-up dynamics, and the fast response necessary to work under varying loads.

All three reactions [1]–[3] can be carried out over industrial Cu/ZnO/Al_2O_3 type catalysts (3–7) with high activity for CH_3OH conversion and very high selectivity for hydrogen production. For these catalytic systems, under flow reaction conditions, the local atomic structure of the surface is itself controlled by the oxidation reaction, since factors such as temperature and gas composition will determine the kinetically controlled response of the catalyst to the reaction conditions. Several authors (8–10) have shown that in POM, both methanol conversion and the concentration of products in the exit stream become strongly dependent on the O_2 concentration in the gas phase.

Although the exact nature of the active sites involved in the production of hydrogen from methanol is still unclear, there is no doubt concerning the major role of surface redox properties ($Cu^{2+}/Cu^{+}/Cu^{0}$) of the catalyst in its reaction behaviour. In general, the standard method for determining the activity and performance of copper-containing catalysts includes a reductive pretreatment in a diluted hydrogen

---

[1] To whom correspondence should be addressed. Fax: +34 1 585 4760. E-mail: jlgfierro@icp.csic.es.

0021-9517/02 $35.00

steam carried out *in situ* and prior to activity measurements. The reduction pretreatment controls the structural and morphological characteristics of the catalyst surface (11–14). These initial characteristics play a central role in the evolution of the oxidation state and structural morphology during the reaction since, as stated above, the dynamic behaviour of the catalyst surface is determined by the gas atmosphere conditions under reaction.

Because the reduction potential of the reactive environment changes the structural and chemical properties of the surface layer, study of the start-up of the reforming over $Cu/ZnO/Al_2O_3$ catalysts in different initial states provides important practical information regarding the activation and handling of catalysts, considering the service expectations of automobile users. With this aim, here we investigated aspects related to the cold start-up behaviour of the methanol reformer for the production of hydrogen over a $Cu/ZnO/Al_2O_3$ catalyst in oxidised, reduced, or reduced + air-exposed forms. In addition, and bearing in mind that a typical catalytic system for automobile applications will be subjected to hundreds of start-up/shut-down cycles in which the catalysts will be exposed to temperature-induced changes in the gas-phase reduction potential, the impact of repeated start-ups and shutdowns on the overall reactor performance is another aspect addressed.

2. EXPERIMENTAL

2.1. *Catalyst Preparation and Characterization*

The copper–zinc–aluminium catalyst (nominal composition $Cu:Zn:Al = 55:40:5$ wt%) was prepared according to the well-documented technique of carbonate co-precipitation from aqueous nitrate solutions of Cu, Zn, and Al, using Na_2CO_3 as a precipitating agent. The solution with the three metal nitrates and the Na_2CO_3 solution were added, both at 0.83 mL/min, to a vigorously stirred $NaHCO_3$ solution at 333 K. During the process, the temperature (333 K) and pH (8.2) of the precipitating solution were strictly controlled. All reagents were used as received: $Cu(NO_3)_2 \cdot 3H_2O$ from Panreac (ACS reagent), $Zn(NO_3)_2 \cdot 6H_2O$ (ACS reagent) from Panreac, $Al(NO_3)_3$ from Fluka (puriss. p.a.), Na_2CO_3 from Panreac (puriss p.a.), and $NaHCO_3$ from Fluka (microselect reagent). The precipitates were aged with stirring for 90 min at 333 K, then filtered, and extensively washed with deionized water at 333 K until the concentration of Na^+ ions in the filtrate solution was lower than 0.1 ppm, as determined by inductively coupled plasma emission spectrometry. The precipitate was dried overnight at 383 K and calcined in air at 623 K for 6 h. Finally, the samples were pelletized and sieved (0.42–0.50 mm) for the catalytic runs. The fresh oxidised sample was characterised by X-ray diffactometry according to the step-scanning procedure (step size 0.02°) using a computerised Seifert XRD 3000P diffractometer (Cu $K\alpha$ radiation; $\lambda = 0.15418$ nm), a PW Bragg-Brentano $\Theta/2\Theta$ 2200 goniometer, equipped with a bent graphite monochromator and an automatic slit. The volume-averaged crystallite sizes of CuO were determined from the half-width of the CuO (111) diffraction line at $2\Theta = 38.8°$ applying the Debye–Scherrer equation. The chemical composition of the catalyst was determined by inductively coupled plasma atomic emission spectroscopy (ICP-AES) using a Perkin–Elmer Optima 3300DV apparatus. The samples were solubilized in a solution of HF, HCl, and HNO_3 and homogenised in a microwave oven at a maximum power of 650 W. Aliquots of the solution were diluted in order to reach a concentration of the elements within the calibration range of the instrument. The nitrogen adsorption–desorption isotherms were obtained at 77 K over the whole range of relative pressures, using a Micromeritics ASAP 2100 automatic device on samples previously outgassed at 523 K. BET surface areas were computed from these isotherms using the BET method and taking a value of 0.1620 nm^2 for the cross section of the physically adsorbed N_2 molecule. Table 1 shows the chemical composition (expressed as weight percentage), particle size of the CuO crystallites, and the textural parameters of the $CuO/ZnO/Al_2O_3$ sample in oxidised form.

2.2. *Catalytic Activity in Temperature-Programmed Start-Ups*

The samples, in oxidised, reduced, and reduced + air-exposed forms, were tested in the temperature-programmed partial oxidation of methanol ($O_2/CH_3OH = 0.3$) using a fixed-bed flow reactor at atmospheric pressure. Temperature-programmed start-up tests were carried out using 0.1 g of calcined sample diluted with SiC (both in the 0.42–0.5 mm particle size range) at a volume ratio of 2 : 1 in order to avoid adverse thermal effects (12). The catalyst bed was placed in a 6-mm I.D. quartz tubular reactor with a coaxially centred thermocouple. Prior to reaction, the catalysts were flushed in nitrogen at 423 K for 2 h followed by: (i) nonadditional pretreatment (oxidised sample) or,

TABLE 1

Chemical Composition, CuO Particle Size, and Textural Properties of the $CuO/ZnO/Al_2O_3$ Oxidised Catalyst

Cu/Zn/Al ratio (wt%)[a]			BET[b] (m^2/g)	Pore diam.[b] (nm)	Dp[c] CuO (nm)
Cu	Zn	Al			
57.8	37.9	4.3	80.1	18.0	4.1

[a] Determined by ICP.

[b] BET specific area and average pore diameter as measured by N_2 adsorption–desorption isotherms at 77 K.

[c] Determined by XRD using the Scherrer equation for CuO ((111) – 38.8°).

(ii) reduction *in situ* at 548 K (heating rate 5 K/min) with 55 mL(STP)/min of 10 vol% H_2/N_2 mixture for 2 h (prereduced sample) or, (iii) reduction by method (ii), followed by catalyst exposure to air at ambient temperature for 24 h (prereduced + air-exposed sample). The pretreating gases were flushed from the reactor with N_2 before admission of the methanol–oxygen–nitrogen reaction mixtures. Methanol was fed into the preheater by means of a liquid pump (Becton–Dickinson) before being mixed with the oxygen and nitrogen streams. Gas flows were adjusted with Brooks model 5850E mass flow controllers. For the POM reaction, the reactants were introduced into the reactor at a molar ratio of $O_2/CH_3OH = 0.3$, using air as oxidant agent. In the catalytic tests, total flow rate was kept at 25 mL(STP)/min (GHSV = 13570 h^{-1}) and the methanol concentration in the feed gas mixture was fixed at 45 vol%. For the start-up measurements, the reaction temperature was programmed according to the following sequence: starting at 423 K for 1 h, subsequent heating at a rate of 0.1 K/min up to 573 K, and finally application of this temperature for 3 h. Taking into account the residence time (0.1 s) used in the experiments, the slow temperature rise (0.1 K/min) was selected to ensure isothermal behaviour of the reactor.

The reaction products were analysed online by GC with TCD (Varian chromatograph, Model Star 3400 CX) equipped with Porapack Q (CO_2, water, methanol, formaldehyde, methyl formate, formic acid, and dimethyl ether), and molecular sieve 5-Å (H_2, O_2, N_2, CO) packed columns connected in series, using He as carrier gas. The composition of the product gas was determined at time intervals of 30 min (3 K in the temperature programme of the reaction). The methanol conversion and product selectivities are based on mole percentages.

3. RESULTS

3.1. Temperature-Programmed Start-Up over Oxidized, Prereduced, and Prereduced + Air-Exposed Samples

The influence of temperature on the activity of the $Cu/ZnO/Al_2O_3$ catalyst in its oxidised, reduced, and reduced + air-exposed forms during the temperature-programmed POM start-up is shown in Fig. 1. For all the pretreatments applied, the methanol conversion profile follows a typical sigmoid-like shape, with a drastic increase in methanol conversion within a narrow temperature range. For the prereduced sample, methanol conversion started at 416 K, while for the prereduced, air-exposed, and oxidised samples this point shifted to higher temperatures: 422 and 434 K, respectively. Both reduced samples, with/without air exposure, displayed the same activity profiles in the whole temperature range, with a temperature shift to slightly higher values in the case of the air-exposed sample. For the unreduced catalyst sample, the activity behaviour of the sample was quite different from that observed for the prereduced counterparts. The oxidised sample behaved similarly, but with lower conversion values than the prereduced samples at temperatures up to about 513 K. At higher temperatures, the increase in methanol conversion induced by the increase in temperature occurred more quickly over the oxidised sample than over the prereduced counterparts. Thus, at temperatures over 521 K, the methanol conversion achieved on the oxidised catalyst surpassed the values corresponding to the prereduced samples.

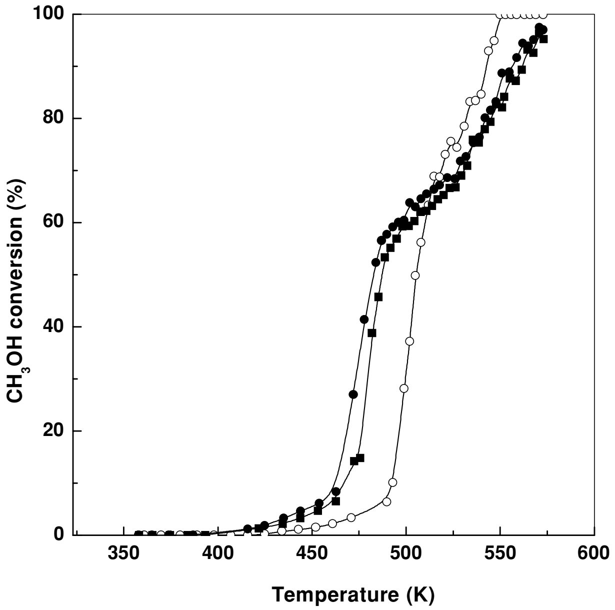

FIG. 1. Temperature dependence of methanol conversion during temperature-programmed start-up over the $Cu/ZnO/Al_2O_3$ catalyst in different initial states: (○) oxidised, (●) reduced, and (■) reduced + air-exposed. Start-up conditions: atmospheric pressure, feed ratio $O_2/CH_3OH = 0.3$, ramp rate = 0.1 K/min.

The conversion patterns for oxygen, Fig. 2, followed the same trend as those observed for the conversion of methanol. Complete conversion of oxygen was reached at 485 K for the prereduced samples and at 512 K for the oxidised sample. The evolution of product selectivity shown in Fig. 2 indicates the existence of several pathways that contribute to the overall reaction. Three ranges of temperature (I, II, III), with characteristic product distributions, can be identified in Fig. 2. In range I (423–460 K), the reaction begins with the formation of formic acid, methyl formate, H_2O, and CO_2. In this temperature window, the rise in temperature was accompanied by an increase in the selectivity of water and CO_2 at the expense of oxygenated compounds. A second temperature-dependent kinetic region was defined in range II (460–500 K). In this region, the reaction developed with a sharp decrease in the selectivity of water, with a simultaneous increase in hydrogen

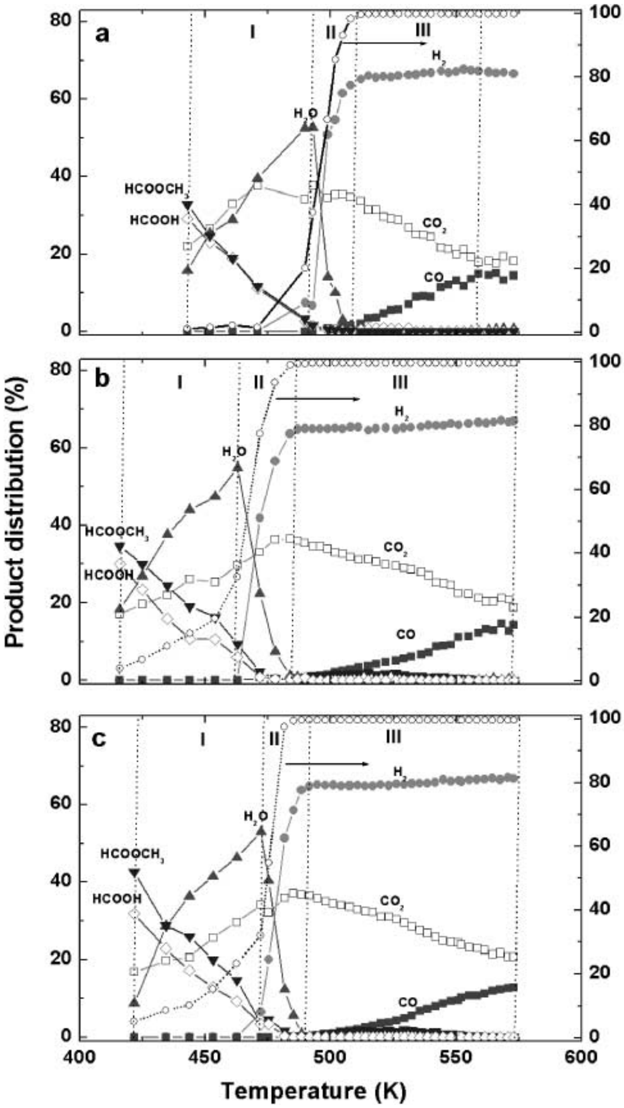

FIG. 2. Temperature evolution of the products: (▲) H_2O, (●) H_2, (□) CO_2, (■) CO, (▼) $HCOOCH_3$, (◇) HCOOH, and (○) O_2 conversion during temperature-programmed start-up over the Cu/ZnO/Al_2O_3 catalyst in different initial states: (a) oxidised, (b) reduced, and (c) reduced + air-exposed. Three temperature ranges: I, II, and III, with characteristic product distributions, were included (see text). Start-up conditions: atmospheric pressure, feed ratio $O_2/CH_3OH = 0.3$, ramp rate = 0.1 K/min.

and CO_2 selectivities. Finally, in range III ($T > 500$ K), the reaction evolved with unchanged H_2 selectivity, accompanied by a steady increase in the CO/CO_2 selectivity ratio with temperature. The same selectivity patterns were observed for all the catalytic samples, irrespective of the initial state. Only the transition temperature that produced the change in the reaction regime depended on the pretreatment applied to the sample. For the prereduced sample, the transition temperatures were set at 463 and 487 K, while for the reduced + air-exposed and oxidised samples the temperatures shifted to 472–491 K and 493–512 K, respectively.

3.2. *Temperature-Programmed Start-Up/Shut-Down/Restart Cycle over an Oxidised Sample*

To know how the working conditions might affect the initial performance of the oxidised catalyst, a second start-up was performed. For this, after the first start-up measurement, the reactor temperature was lowered under a static reactive atmosphere from 573 K to room temperature. Once cooling was complete, the second start-up was performed, following the temperature protocol defined in the experimental section for the start-up of the reformer. Figure 3 compares the methanol conversion profile of the oxidised sample subjected to the start-up/shut-down/restart-up cycle. The product distribution obtained over the oxidised sample during this cycle is shown in Fig. 4. The experimental data point to considerable differences in catalytic behaviour between the first and second start-ups. During the second cycle, a measurable methanol conversion was observed at a significantly lower temperature (465 K). Above this temperature, the methanol conversion achieved during the second start-up was lower than that attained during the first start-up.

3.3. *Consecutive Start-Up/Shut-Down Cycles*

To estimate the impact of repeated start-ups and shut-downs on the overall catalyst performance, the effect of

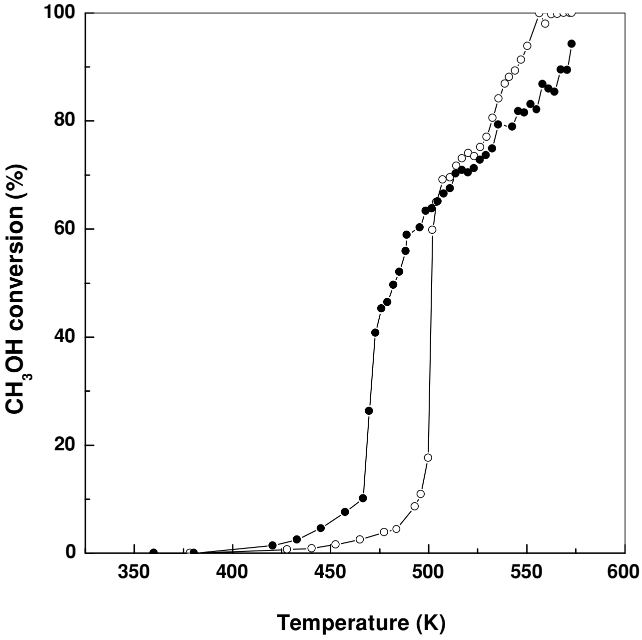

FIG. 3. Temperature dependence of methanol conversion over the sample in the oxidised initial state during temperature-programmed start-ups following the cycle: (○) first start-up/shut-down/ (●) consecutive start-up.

temperature cycles was investigated. For this purpose, after a temperature-programmed reaction over the catalyst in the oxidised state, the catalytic bed was subjected to shut-down procedures, varying the length of the stand-by period. During the different shut-downs, the sample was cooled to room temperature under a static reactive atmosphere, remaining under this atmosphere for 4, 72, and 96 h. After these stand-by periods, the activity was evaluated again in accordance with the reactor temperature programme described previously. Figure 5 shows the changes in CH_3OH conversion during the cycled temperature-programmed reaction after catalyst stand-by operations for periods of 4, 72, and 96 h. A negligible effect, neither methanol conversion nor product distribution were seen for stand-by periods under the reactive atmosphere of less than 72 h. Only for the catalyst subjected to a stand-by period of 96 h was the onset of the reaction shifted to a slightly higher temperature.

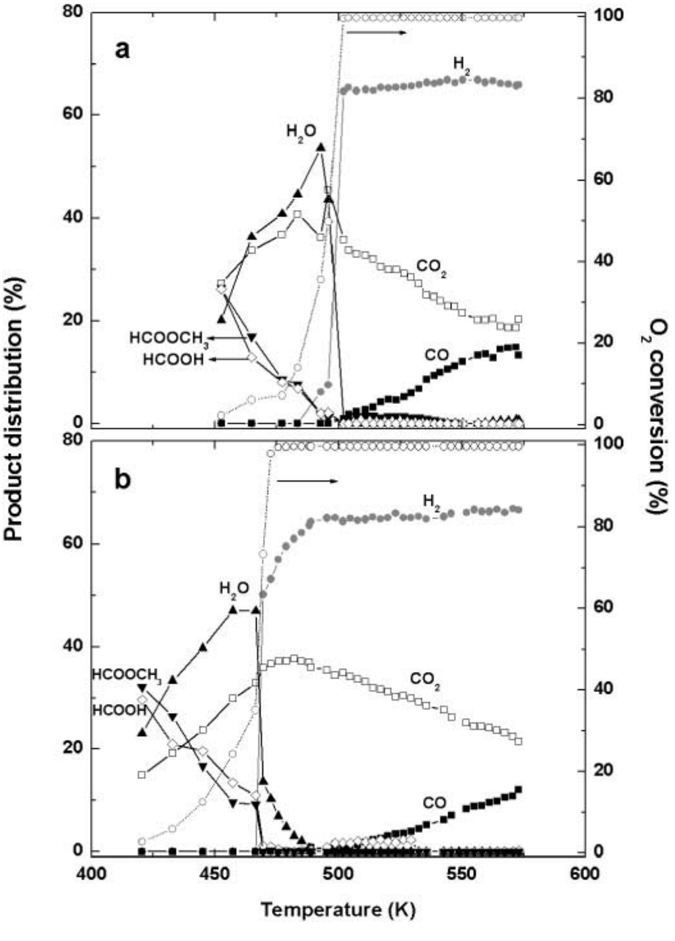

FIG. 4. Evolution with temperature of the reaction products: (▲) H_2O, (●) H_2, (□) CO_2, (■) CO, (▼) $HCOOCH_3$, (◇) HCOOH, and (○) O_2 conversion over the sample in the oxidised initial state during temperature-programmed start-ups following the cycle: (a) first start-up/shut-down/ (b) consecutive start-up.

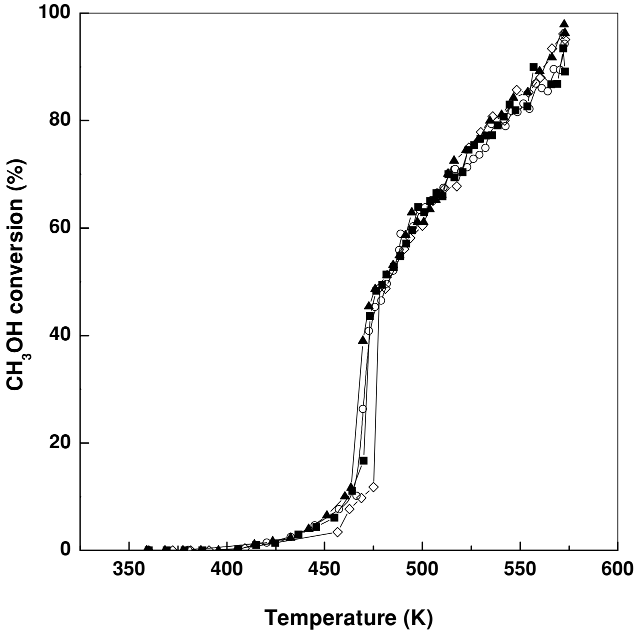

FIG. 5. Temperature dependence of methanol conversion for POM during temperature-programmed cyclic start-ups after stand-by periods under a static reactive atmosphere of different durations: (▲) 0 h, (○) 4 h, (■) 72 h, and (◇) 96 h.

4. DISCUSSION

4.1. Influence of the Initial State of the Catalyst on the Start-Up Behaviour of the Reformer

The product selectivity patterns (Fig. 2) clearly indicate that the same potential reaction networks (9) operate for the catalyst in reduced, air-passivated, or oxidised forms. Only the profile of methanol conversion and the onset temperatures for each chemical region that contributes to the overall conversion vary with the pretreatment applied.

In the case of prereduced samples, it is evident that the reduced/oxidised catalyst state is affected by the kinetics of the catalytic reaction since the catalytic reactions involved in POM consume oxygen in competition with copper oxide formation:

$$4Cu + O_2 \rightarrow 2Cu_2O. \quad [4]$$

At low reaction temperatures, the prereduced sample is expected to be oxidised at surface level by gas oxygen according to reaction [4]. Reitz *et al.* (8) and Günter *et al.* (10) observed by time-resolved XANES Cu^+ as transient species at low temperatures under reaction flow over reduced Cu/ZnO samples. However, some authors (16)—taking into account the low O_2/CH_3OH molar ratio used and the mismatch between the lattice parameters of cubic Cu and Cu_2O—have indicated that complete oxidation of the surface is not to be expected, as indicated by Eq. [4], its being more plausible for there to be a two-dimensional copper suboxide surface species. The exposure of the prereduced sample to air for 24 h leads to an increase in the abundance of these suboxidized structures, with the development of Cu_2O structures, but maintaining the Cu^o core particle (17, 18). In the case of the oxidised sample only CuO surface species are present.

Besides chemisorbed oxygen, the reactions involved in the beginning of partial oxidation of methanol require the existence of metal sites. It is evident that higher degrees of surface oxidation in the samples induce a shift to higher values in the reaction temperature at which the reaction starts (see Fig. 1). To explain this behaviour, the ability of the surface to promote the adsorption of CH_3OH must be taken into account. Several studies (19, 20) have pointed to the importance of the amount of oxygen at the surface in the probability of methanol sticking to copper atoms. In these studies, it was demonstrated that the methanol sticking probability was enhanced at low oxygen coverage, while at high oxygen coverage the sticking probability decreased. Therefore, lower methanol conversion is expected when the extent of surface oxidation increases. In the case of oxide surfaces, the metal sites are difficult to access due to the inherently large size of oxygen ions relative to cations. Defects in closed-packed surfaces and incompletely coordinated oxide polyhedra are, however, accessible for the chemisorption of adsorbates being able to deprotonate methanol to methoxide (21). In this case, the exposed Cu cations and oxide anions behave as Lewis acid and Brønsted conjugate base sites. Once the reaction begins, the oxygen is continuously consumed by reaction with CH_3OH, the surface being progressively activated by increasing numbers of defects generated by the reaction itself (22). Therefore, at high oxygen coverage the reaction starts with a low reaction probability but increases as more vacancies are created in the oxygen layer.

The change in reaction product with temperature (Fig. 2) indicates the sensitivity of the mechanism to the local atomic structure, which is itself controlled by the reaction. In keeping with this, the reaction evolution is accompanied by surface/bulk reduction/reconstruction. The high concentration of oxygen adatoms at the first steps of the reaction allows the evolution of the superficial methoxide toward products of total oxidation. In all cases, methanol conversion by total oxidation does not reach its maximum stoichiometric value (20% for O_2/CH_3OH ratio of 0.3), a maximum value—irrespective of catalyst pretreatment—of 9% being achieved. The high stoichiometric amount of O_2 required for the total oxidation of methanol entails a fast decrease of the O_2 content in the gas. This increase in the reducing potential of the gas phase, together with the excess of energy, implies a progressive removal of surface oxygen species, which favours the dehydrogenation pathway under substoichiometric amounts of surface oxygen. When all oxygen available for oxidation has been consumed (60% of methanol conversion for $O_2/CH_3OH = 0.3$), the excess of methanol is converted through the endothermic decomposition pathway on metallic Cu atoms (23, 24).

The higher activity shown by the oxidised sample once the reaction has started points to the different evolution of the catalyst surface under the reaction conditions of this sample with respect to the prereduced counterparts. Variations in the surface structure of Cu in Cu/ZnO catalysts due to changing either the reducing agent or the reduction conditions have been previously described in the literature (11, 12, 14). Changes in the relative abundance of different crystallographic Cu metal planes (12), the formation of Cu–Zn alloys (13), or the coalescence of copper crystallites (25) induced by the exothermicity of reduction may be involved in the differences in catalytic activity found as a result of changes in the reduction/reaction conditions. In spite of the differences in reactivity found for the samples tested, analysis of the products versus methanol conversion reveals that the product distribution at an equal value of methanol conversion does not depend significantly on the pretreatment applied to the sample. Only for the oxidised sample is the participation of the reverse water gas-shift reaction observed when practically all the methanol has been converted. The absence of marked differences in product distribution at methanol isoconversion strongly suggests that the differences in activity between oxidised and prereduced samples can be ascribed to a change in the number, but not in the characteristics, of the active sites induced by the different reduction potentials of the reacting gases. Therefore, it is feasible to propose that Cu is more dispersed or that its dispersion is more stabilised when the starting up of the reformer is performed over the catalysts in oxidised form rather than in prereduced form. Further work concerning this relationship will be carried out in the future.

4.2. *Consecutive Start-Up/Shut-Down Cycles over an Oxidised Sample*

As shown in Fig. 3, a different methanol conversion profile was obtained when the sample in oxidised state was subjected to a consecutive start-up. During the second start-up the reaction began at a lower temperature, displaying a conversion profile and product distribution identical to those of the prereduced sample, thus confirming the reduction of the catalysts under reaction. As has been pointed out above, it appears reasonable to assume that the surfaces developed under reaction on oxidised samples are different from those developed on prereduced counterparts. In spite of these structural differences at the beginning of the reaction, both the prereduced sample and the reaction-reduced counterpart showed the same activity behaviour (Figs. 1 and 3). The surface changes at high temperature under a reducing atmosphere have been associated with either the sintering of copper (25) or the migration of ZnO_x onto the Cu surface (13, 26). These phenomena could be the origin of the differences found between the first and the consecutive start-ups over the oxidised sample. This interpretation is, however, inconsistent with the fact that the catalyst maintained at 573 K for 3 h did not show evidence of deactivation. Additionally, the absence of thermal sintering effects associated with the experimental protocol is supported by the consecutive start-ups carried out over the reaction-reduced sample, in which activity remained virtually unchanged (Fig. 5). Therefore, the differences found between both prereduced and reaction-reduced catalysts and the oxidised counterpart must be related to the lattice oxygen present in the latter. The question as to how the lattice oxygen present in the oxidised sample influences the structural changes occurring under reaction and the reason these changes lead to higher catalytic activities in methanol decomposition remain obscure and require further investigation.

5. CONCLUSIONS

The temperature-programmed start-up of the reformer for hydrogen production by POM using a feed molar ratio of $O_2/CH_3OH = 0.3$ was studied under $Cu/ZnO/Al_2O_3$ catalysts in oxidised, reduced, and reduced + air-exposed forms. The importance of the initial state of the catalyst in the start-up behaviour of the reformer was demonstrated. The profile of methanol conversion and the onset temperatures for each chemical region contributing to the overall conversion differ, depending on the initial state of the catalyst. Oxidative dehydrogenation and combustion are faster over the prereduced samples. Passivation of samples by contact with air at room temperature only slightly retards the start of the reaction. The reduction of oxidised sample takes place under reaction and leads to a surface reconstruction with a higher methanol decomposition capacity than those derived from reduction pretreatments. The higher decomposition capacity found for the oxidised sample is most likely related to differences in the number, but not in the characteristics, of the active sites induced by the different reduction potentials of the reacting gases. The differences in surface features shown by the oxidised sample under the first reaction are not maintained during the second start-up. In this case, the reaction-reduced catalyst behaves identically to the prereduced counterpart. A negligible effect on methanol conversion during repeated start-up and shut-down cycles over the oxidised sample is observed. Consequently, the prereduction of the $Cu/ZnO/Al_2O_3$ catalyst is not necessary for high conversion and selectivity for H_2 production in POM reactions to be achieved. This may have important implications in reformers for automobile use since no additional equipment included to activate the catalyst would be necessary.

ACKNOWLEDGMENTS

Financial support of this work from the European Regional Development Fund under Contract 2FD97-1405-C02-01 is acknowledged. RMN gratefully acknowledges financial support (I3P-PC2001-2 programme) from the European Social Fund.

REFERENCES

1. Peschka, W., *Int. J. Hydrogen Energy* **23**, 27 (1998).
2. Trimm, D. L., and Önsan, Z. I., *Catal. Rev.* **43**(1–2), 31 (2001).
3. Takahashi, K., Takezawa, N., and Kobayashi, H., *Appl. Catal.* **2**, 363 (1982).
4. Amphlett, J. C., Evans, M. J., Mann, R. F., and Weir, R. D., *Can. J. Chem. Eng*. **63**, 605 (1985).
5. Alejo, L., Lago, R., Peña, M. A., and Fierro, J. L. G., *Appl. Catal., A* **162**, 281 (1997).
6. Agrell, J., Hasselbo, K., Jansson, K., Järäs, S. G., and Boutonnet, M., *Appl. Catal., A* **211**, 239 (2001).
7. Mizsey, P., Newson, E., Truong, T., and Hottinger, P., *Appl. Catal., A* **213**, 233 (2001).
8. Reitz, T. L., Lee, P. L., Czaplewski, K. F., Lang, J. C., Popp, K. E., and Kung, H. H., *J. Catal.* **199**, 193 (2001).
9. Murcia-Mascarós, S., Navarro, R. M., Gómez-Sainero, L., Costantino, U., Nocchetti, M., and Fierro, J. L. G., *J. Catal.* **198**, 338 (2001).
10. Günter, M. M., Ressler, T., Jentoft, R. E., and Bems, B., *J. Catal.* **203**, 133 (2001).
11. Grunwaldt, J. D., Molenbroek, A. M., Topsøe, N. Y., Topsøe, H., and Clausen, B. S., *J. Catal.* **194**, 452 (2000).
12. Sakakini, B. H., Tabata Baei, J., Watson, M. J., and Waugh, K. C., *J. Mol. Catal. A: Chem.* **162**, 297 (2000).
13. Topsøe, N. Y., and Topsøe, H., *J. Mol. Catal. A: Chem.* **141**, 95 (1999).
14. Fujita, S.-I., Moribe, S., Kanamori, Y., Kakudate, M., and Takezawa, N., *Appl. Catal., A* **207**, 121 (2001).
15. Mears, D. E., *J. Catal.* **20**, 127 (1971).
16. Knop-Gericke, A., Hävecker, M., Schedel-Niedrig, T., and Schlög, R., *Top. Catal.* **15**(1), 27 (2001).
17. Urban, J., Sack-Kongehl, H., and Weiss, K., *Catal. Lett.* **49**, 101 (1997).
18. Bart, J. C. J., and Sneeden, R. P. A., *Catal. Today* **2**, 1 (1987).
19. Clarke, D. B., Lee, D. K., Sandoval, M. J., and Bell, A. T., *J. Catal.* **150**, 81 (1994).
20. Bowker, M., *Top. Catal.* **3**, 461 (1996).
21. Jones, P. M., May, J. A., Reitz, J. B., and Solomon, E. I., *J. Am. Chem. Soc*. **120**, 1506 (1998).
22. Dadykov, V. A., Tikhov, S. F., and Popovskii, V. V., *Kinet. Katal.* **27**, 133 (1986).
23. Sato, S., Iijima, M., Nakayama, T., Sodesawa, T., and Nozaki, F., *J. Catal.* **169**, 447 (1997).
24. Vanderborg, N. E., Goodby, B. E., and Sringer, T. E., *in* "Proceedings of the 32nd International Power Sources Symposium," p. 623, 1986.
25. Gines, M. J. L., and Apesteguia, C. R., *Latin Amer. Appl. Res.* **25**, 215 (1995).
26. Fujitani, T., and Nakamura, J., *Appl. Catal., A* **191**, 111 (2000).